Proceedings of 2023 IEEE
International Conference on Mechatronics and Automation
August 6 - 9, Harbin, Heilongjiang, China

Fatigue Analysis of Leg Structure of a Natatores-Like Amphibious Robot

Yan Niu[1,3], Liwei Shi[1,3], Shuxiang Guo[1,2,3,4]*

1.School of Medical Technology, Beijing Institute of Technology, Beijing, 100081, China
2.School of Life Science, Beijing Institute of Technology, Beijing, 100081, China
3.Key Laboratory of Convergence Medical Engineering System and Healthcare Technology(Beijing Institute of Technology), Ministry of Industry and Information Technology, Beijing, 100081, China
4.The Department of Electronic and Electrical Engineering, Southern University of Science and Technology, Shenzhen,Guangdong 518055,China

** Corresponding author: shiliwei@bit.edu.cn*

***Abstract* - With the increasing demand for ocean exploration and development, the research about the amphibious robot is of great significance. In this paper, a natatores-like amphibious robot was designed by using the driving method of paddling by webbed foot. This mode has the advantages of high propulsion efficiency, good mobility and good stability. Due to the characteristics of this propulsion mode, the leg structure of the robot is often applied with periodic loads. And therefore it is necessary to verify the mechanical performance of the leg structure. The elastoplastic finite element model of the leg structure of the robot was modelled, and the fatigue analysis of the model under the walking gait were carried out. The results showed that the fatigue failure of the thigh and the shank would not occur within the design life, which met the design requirements. The analysis results can provide reference for the material selection and structural optimization design of leg in the subsequent work.**

Index Terms - Natatores-like amphibious robot, Finite element, Fatigue analysis, ANSYS.

I. INTRODUCTION

Nowadays, with the increasing demand for ocean exploration and development, the robots need to work at shallows, amphibious battlefields and other complex terrains. In addition, the robots are required to be able to successfully carry out some special tasks, such as rescue and relief under geological disasters. So, amphibious robots have become one of the research focuses [1]. The types of traditional amphibious robot mainly include the wheel-propeller robot, the legged robot and so on [2-3]. While the robots mentioned above have the disadvantages of worse environmental adaptability and more difficulty in controlling.

In recent years, with the development of bionics, bionic propulsions have gradually become the prime selections of amphibious robots [4-6]. There are many types of amphibians in nature which can inspire scholars to develop various robots with different propulsions. Yan et al [7] proposed a bionic fairing inspired by hammerhead sharks to reduce navigational resistance and energy consumption and to improve the working efficiency of a novel track-propeller composite amphibious robot. Chen et al [8] inspired by the crab by the sea, they presented an amphibious robot that combines walking and swimming move modes. This team also developed a calculation approach for the kinematics of the leg which was applied on the crab-like robot. After optimize ,the stride length of walking has greatly increased [9]. For sampling and ultrasonic drilling tasks of seabed rocks, Li et al [10] proposed a novel underwater robot whose structure is inspired by soft jellyfish. The robot can move flexibly and stably with low noise, outstanding cruising ability and strong environmental adaptability. Cheng et al [11] also presented an umbrella jellyfish bionic robot. They studied the displacement of the jellyfish robot in the same direction and the distribution of surrounding fluid pressure caused by the robot motion under different experimental conditions. Xing et al [12] proposed a amphibious spherical robot inspired by the turtle, which is used to execute exploration missions in the restricted environment. And a real-time tracking system who has high image processing rate was applied on the robot [13]. Shi et al [14-15] used different types of materials, such as shape memory alloy and ionic polymer metal composite to develop bionic robots and make great achievements. Nagai et al [16] developed an antagonistic actuator based on DEAs and applied it on a swimming robot. Graf et al [17] improved the robot based on crab-like legs and tested the performance of it. Baines et al [18] presented a morphing limb inspired by turtle. The structure can adapt the mode switch. In addition, there are still various researches about bionic amphibious robots[19-23].

Among the bionic propulsions, paddling by webbed feet has been selected as the driving mode of the bionic robot because of its high propulsion efficiency, good mobility and good stability [24].

One of the most effective methods to verify whether the selected propulsion mode meets the requirements is mechanical analysis, including static analysis, modal analysis, fatigue analysis, etc [25]. Fatigue failure is a common form of failure. When mechanical components are loaded repeatedly, cracks or permanent deformation will occur in the weak areas. The component will be damaged under the action of circularly loads, even if the stress is less than the allowable stress. Fatigue failure will lead to serious consequences. And therefore fatigue analysis of the key components is of great significance in engineering.

The optimization design of key components can be carried out based on the fatigue life, the damage, the fatigue

sensitivity or other fatigue characteristics obtained by the simulation calculation, which is a common research method.

Du et al [26] put forward a fatigue analysis method based on dynamic stress for flexible robots. The fatigue characteristics of the robot were analyzed and the results were used as references for structural design. Guo et al [27] studied the fatigue characteristics of the circular middle plate and leg brackets of the amphibious spherical robot. The slice gaskets were added at dangerous locations to reduce the risk of fatigue failure and extend the service life. Zhu et al [28] gave improvement suggestions for the bipedal assisted exoskeleton robot according to the analysis results of the fatigue equivalent loads and the fatigue life which were calculated by Finite Element Method. In order to analyze the fatigue life of flexible joint robot under impact force, Nie et al [29] proposed a complete modeling and simulation method. Zhi et al [30] proposed a fatigue reliability analysis technique based on fuzzy design optimization, and then they obtained the optimal fatigue reliability of structures with random parameters under the minimum fatigue life fluctuation.

The above researches can be seen clearly that the fatigue analysis of the pivotal components of the robot has become one of the most important research contents in the robotic field. This paper studies the fatigue characteristics of the leg structure of the designed natatores-like amphibious robot under the walking gait. The results can provide a theoretical reference for the optimization of the material and structure of the robot.

The structure of this paper is as follows. Section II introduces the overall structure and the walking gait design of the natatores-like robot; Section III describes the establishment of the finite element model of leg structure; Section IV analyzes the simulation results of fatigue characteristics of leg structure; Section V describes the conclusion and the future work.

II. Overall Structure And Walking Gait

Mallards have pairs of webbed feet which meet the needs of moving in complex terrain. And therefore the design of the natatores-like amphibious robot is carried out using the method of biological observation of mallards. The structural design of this robot is mainly composed of head-neck design, leg design and body waterproof design. The leg design is the propulsion structure of the robot. The leg structure is shown in Fig. 1. It is composed of the thigh, shank and webbed feet.[31].

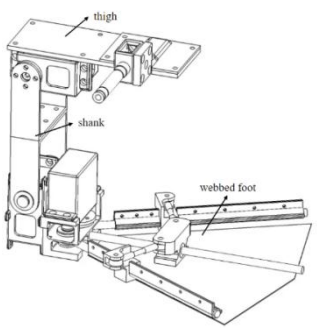

Fig. 1 The leg structure

The analysis of this research mainly focuses on the fatigue characteristics of the leg structure of the robot when walking in the land environment. It takes four seconds to complete each cycle which can be divided into four components, including initial posture, right leg raised posture, left leg raised posture, and standing posture after walking.

III. Fatigue Analysis Modelling Of Leg Structure

The servo motors of the knee joint and ankle joint need to rotate forward and reversely in the situation of walking on land, which cause that the thigh and shank are loaded periodically. So it is necessary to check the performance of them and verify whether the leg structure is reliable when the robot walks on the land. In this research, Finite Element Method(FEM) is used to carry out the simulation analysis. The module of Static Structural of ANSYS workbench software is used for finite element modelling and the Fatigue Tool is used for fatigue analysis.

A. Finite Element Modelling of Leg Structure

The thigh is consisted of three parts, including the swivel structure component of leg, the extension board of leg and the casing of servo motor. Among them, the function of the swivel component of leg is to avoid the interference between the leg structure and the body waterproof. The extension board of leg is used to increase the range of the motion. The casing of servo motor is used to place the motor.

In order to improve the calculation efficiency with the finite element model, the thigh is simplified while the necessary features were retained. There are various types of mesh which can be selected in FEM, such as the tetrahedron, hexahedron, prism, pyramid and so on. The tetrahedron element is widely used because of its good adaptability and quick mesh generation. And therefore this part uses the tetrahedron element with ten nodes.

FEM completes the calculation by using the basic idea of use discrete elements to approximate continuum. The number of the discrete elements has a great influence on the simulation results. Generally speaking the more elements are generated, the more accurate simulation results can be obtained. But if the elements are too much, the cost of computing is enormous. So, it is necessary to find the proper number of discrete elements. This could be verified by calculating the same results with different generating elements. The influence on the results caused by the number of elements can be ignored when the error of results is smaller than 10% between the two adjacent calculations. The independence of mesh is validated through a simple example. The comparison of simulation results with different elements are shown in Table I.

TABLE I
The Maximum Of Equivalent Stress At The Thigh

Number of elements	Result
36742	33.93MPa
53173	34.22MPa
82825	35.91MPa

The mesh size cannot be further reduced due to the structural size. And the numbers of elements shown in Table II are selected. The percentage difference between the two with 36742 elements and 82825 elements respectively is 5.5%. This

error is acceptable. So, totally the 36742 elements and 67717 nodes are divided successfully. Fig.2 shows the finite element model of the thigh. The thigh model applies binding constraints which play the role of bolts on the contact surfaces of the three parts. Degrees of freedom of translation of the hip joint and the knee joint are constrained. The maximum torque of the knee joint is 1.6Nm obtained by the kinetics calculation which is simulated in ADAMS software. The constant amplitude symmetrical cyclic load is applied to the knee joint. The amplitude is the maximum torque in the knee joint. The stress ratio which is defined as the ratio of the minimum to maximum is -1.

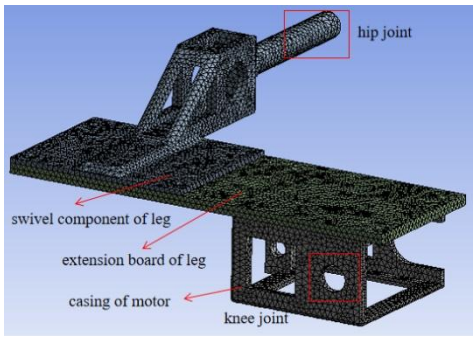

Fig. 2 Three dimensional elastoplastic finite element model of thigh

The shank is composed of two U-shaped plates connected by bolts which can increase the stiffness and decrease the deformation. The element type also adopts tetrahedron. The mesh independent validation is also carried out and the comparison of results is shown in Table II.

TABLE II
THE MAXIMUM OF EQUIVALENT STRESS AT THE SHANK

Number of elements	Result
13462	32.46MPa
105675	41.99MPa
801725	42.87MPa

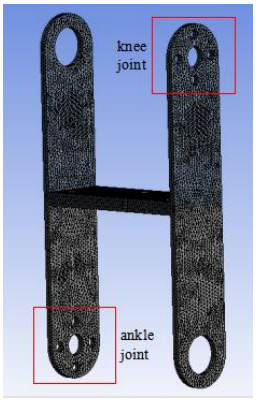

Fig. 3 Three dimensional elastoplastic finite element model of shank

The percentage difference between the two with 105675 elements and 801725 elements is 2.1%. It can be verified that the simulation results are not related to the number of the mesh when the number is greater than 105675. So the shank is divided into 171480 nodes and 105675 elements. Fig.3 shows the finite element model of the shank. Binding constraints are also applied on the contact surface between two U-shaped plates. Degrees of freedom of translation of the output shaft of the servo motors are constrained at both the knee joint and the ankle joint. The maximum torque of the ankle joint is 1.1Nm which is also obtained by simulation in ADAMS. And the method of loading at the knee joint and the ankle joint of the shank is the same as the one at knee joint of thigh.

B. Material Property

The thigh and shank of the robot use 45# steel. The material properties are shown in Table III.

TABLE III
THE MATERIAL PROPERTIES OF 45# STEEL

Density	7890kg/m^3
Young's Modulus	209GPa
Poisson's Ratio	0.269
Yield Strength	335MPa

The type of fatigue can be divided into high-cycle fatigue and low-cycle fatigue according to the number of cycles causing failure. When the number of cycles is greater than 10^4, the fatigue is called high-cycle fatigue. In this case, the cyclic stress applied on the structure is less than the yield limit of the material and only the elastic strain occurs. If the number of cycles is smaller than 10^4, the fatigue is called low-cycle fatigue. In this case, the cyclic stress is higher than the yield limit and both the elastic and plastic strain occur.

High-cycle fatigue is selected to analyze the fatigue characteristics of the leg structure, so it is necessary to define the S-N curve of the materials. This curve represents the relationship between fatigue strength and life of standard sample under certain cycle. The mathematical expression of this curve is shown in(1)

$$LgS = A + BLgN$$

where S represents the stress, N represents the number of cycles, A and B are constants.

Fig.4 shows the S-N curve of 45# steel, which is expressed in the form of double logarithm. The data under the hardness of 210HV is selected [32]. The fatigue limit of 45# steel under this hardness is 147Mpa. The influence of mean stress is not considered in this paper. And the fatigue strength factor is 0.8.

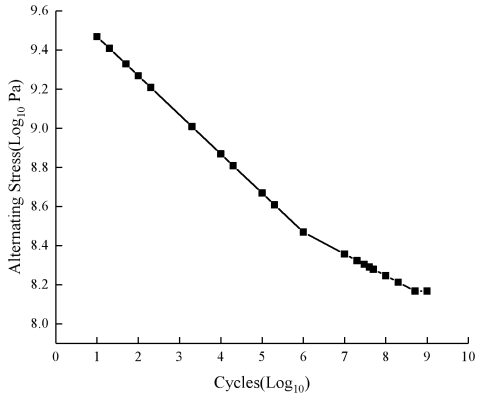

Fig. 4 S-N curve of 45# steel

IV. ANALYSIS OF FATIGUE SIMULATION RESULTS

Fatigue analysis is carried out based on the above finite element models. This section will analyze the damage, equivalent alternating stress, safety factor and fatigue sensitivity of the thigh and shank.

A. Thigh

Damage is defined as the ratio of the design life to the actual service life. When the value is less than 1, it means that fatigue failure will not occur when the part is used within the design life. Otherwise there is a hidden danger of fatigue failure. The maximum damage of the thigh is 0.1 according to simulation results. So there is no risk of fatigue failure for the thigh within the design life.

The safety factor represents the ratio of the failure stress to the design stress. The value of safety factor must be greater than 1 so that the component meets the design requirements. Fig.5 shows the the simulation results of the safety factor of the thigh. The minimum is 4.1557, which occurs at the surface where the symmetrical cyclic load is applied. The safety factor is greater than 1, so the thigh meets the design requirements.

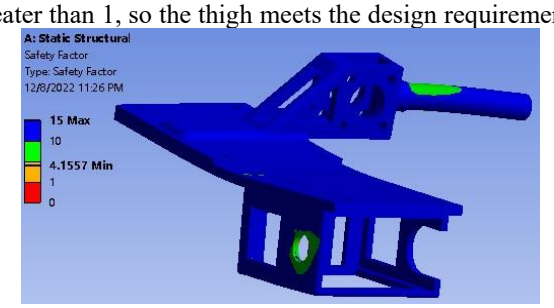

Fig. 5 The safety factor of the thigh

Fig.6 shows the distributing graph of equivalent alternating stress of the thigh. The maximum is 42.408MPa, and the location is the same as the location where the maximum of safety factor occurs. This value is less than the fatigue limit of 45# steel, so the maximum life of thigh is 10^9 cycles.

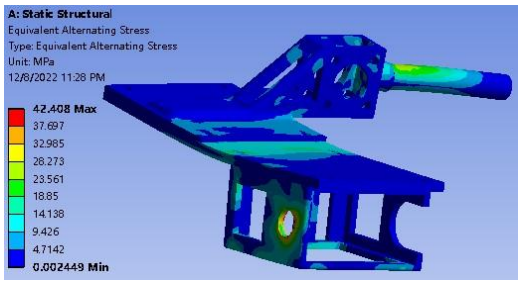

Fig. 6 Distributing graph of equivalent alternating stress of the thigh

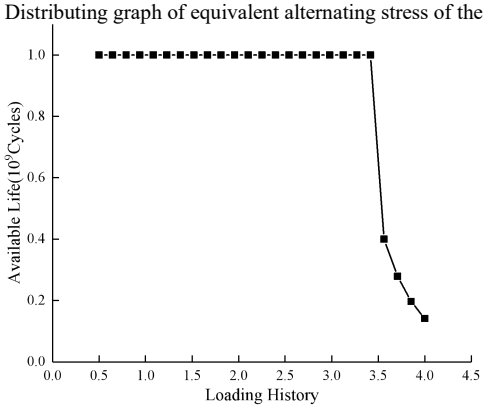

Fig. 7 Fatigue sensitivity of the thigh

The curve of fatigue sensitivity shows the minimum available life of the component with the increase of the multiple of applied load. Fig.7 shows the simulation results of fatigue sensitivity of thigh. The horizontal axis represents the multiple of applied load. It can be seen that with the increase of load, the available life of thigh is mainly 10^9 cycles. When the loading multiple is 3.56, the life starts to decrease, so the thigh is safe.

B. Shank

The damage of the shank is also 0.1 according to fatigue simulation results. It indicates that the fatigue failure will not occur within the design life. Fig.8 shows the the simulation results of the safety factor of the shank. The minimum is 3.3557, which occurs at the surface between the shaft of servo motor at knee joint and the U-shaped plates. This value is greater than 1, so the shank meets the design requirements.

Fig.9 shows the distributing graph of equivalent alternating stress of the shank. The maximum is 52.486Mpa. Because the amplitude of load applied at the knee joint is greater than that at the ankle joint, the maximum occurs at the knee joint. However, this value is still less than the fatigue limit. So the maximum life of the shank is 10^9 cycles.

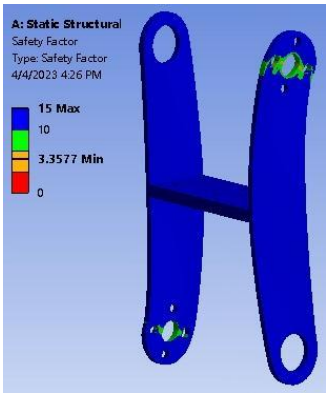

Fig. 8 The safety factor of the shank

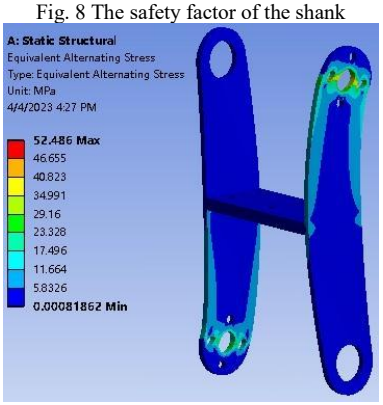

Fig. 9 Distributing graph of equivalent alternating stress of the shank

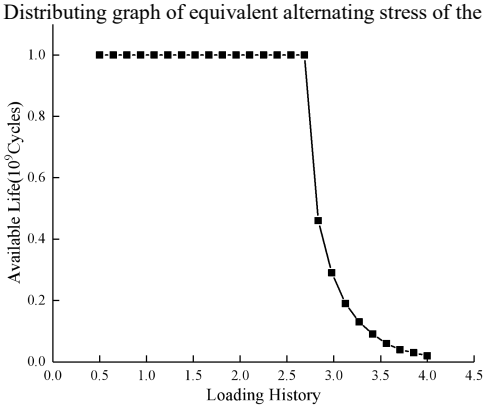

Fig. 10 Fatigue sensitivity of the shank

Fig.10 shows the fatigue sensitivity of shank. With the increase of multiple, the available life of shank is also mainly 10^9 cycles, and it will decrease after 2.83 times of the applied load. So the shank is safe.

V. Conclusion And Future Work

This paper carried out fatigue analysis of thigh and shank when the natatores-like amphibious robot walked on the land. Several fatigue characteristics were analyzed. The results showed that the fatigue failure would not occur at the thigh and the shank when they were used within the design life, which met the design requirements.

In this paper, the results of fatigue analysis could provide a theoretical reference for the optimal design of materials and structures for leg. In addition, this paper only analyzes the fatigue characteristics of leg structure under the walking gait. The subsequent work should continue to verify the fatigue characteristics of leg structure when robot moves underwater.

Acknowledgment

This work was supported by National Natural Science Foundation of China (62273042, 61773064).

References

[1] J. Zhang, J. Zhou, S. Yuan and C. Jing, "Review of configuration, motion mechanism, modeling and control of amphibious bionic robots," *Robot*, in press.

[2] X. Bai, J. Shang, Z. Luo, T. Jiang, and Y. Qian, "Development of amphibious biomimetic robots," *Journal of Zhejiang University-Science A (Applied Physics & Engineering)*, vol. 23, no. 3, pp. 157-187, March 2022.

[3] K. Ren, and J. Yu, "Research status of bionic amphibious robots: A review," *Ocean Engineering* , vol. 227, no. 3, pp. 108862, March 2021.

[4] Y. Meng, Z. Wu, H. Dong, J. Wang, and J. Yu, "Toward a novel robotic manta with unique pectoral fins," *IEEE Transactions on Systems, Man, and Cybernetics: Systems*, vol. 52, no. 3, pp. 1663-1673, March 2022.

[5] B. Han, X. Luo, X. Wang, and X. Chen, "Mechanism design and gait experiment of an amphibian robotic turtle," *Advanced Robotics*, vol. 25, no. 16, pp. 2083-2097, April 2011.

[6] A. Boxerbaum, M. Klein, J. Kline, S. Burgess, R. Quinn, R. Harkins, and R. Vaidyanathan, "Design, simulation, fabrication and testing of a bio-inspired amphibious robot with multiple modes of mobility," *Journal of Robotics and Mechatronics*, vol.24, no. 4, pp. 629-641, August 2012.

[7] Z. Yan, M. Li, Z. Du, X. Yang, Y. Luo, X. Chen and B. Han, "Study on a tracked amphibious robot bionic fairing for drag reduction," *Ocean Engineering*, vol. 267, no. 1, pp. 113223, January 2023.

[8] X. Chen, J. Li, S. Hu, S. Han, K. Liu, B. Pan, J. Wang, G. Wang and X. Ma, "Study on the design and experimental research on a bionic crab robot with amphibious multi-modal movement," *Journal of Marine Science and Engineering*, vol. 10, no. 12, pp. 1804, November 2022.

[9] G. Wang, K. Liu, X. Ma, X. Chen, S. Hu, Q. Tang, Z. Liu, M. Ding and S. Han, "Optimal design and implementation of an amphibious bionic legged robot," *Ocean Engineering*, vol. 272, no. 3, pp. 113823, March 2023.

[10] H. Li, G. Wang, L. Li, M. Wei, Y. Li, W. Sun and Q. Zeng, "Design of the swimming system of a bionic jellyfish robot for seabed exploration," *Applied Ocean Research*, vol. 134, no. 3, pp. 103498, May 2023.

[11] Q. Cheng, W. Mo, L. Chen, W. Ke, J. Hu and Y. Wu, "Numerical study of different engineering conditions on the propulsive performance of the bionic jellyfish robot," *Sustainability*, vol. 15, no. 5, pp. 4186, February 2023.

[12] H. Xing, S. Guo, L. Shi, X. Hou, Y. Liu, H. Liu, Y. Hu, D. Xia and Z. Li, "A novel small-scale turtle-inspired amphibious spherical robot," *2019 IEEE/RSJ International Conference on Intelligent Robots and Systems (IROS)*, pp. 1702-1707, 2019.

[13] S. Guo, S. Pan, X. Li, L. Shi, P. Zhang, P. Guo and Y. He, "A system on chip-based real-time tracking system for amphibious spherical robots," *International Journal of Advanced Robotic Systems*, vol. 14, no. 4, pp. 1-19, July 2017.

[14] L. Shi, S. Guo, K. Asaka, "A novel jellyfish-and butterfly-inspired underwater microrobot with pectoral fins," *International Journal of Robotics and Automation*, vol. 27, no. 3, pp. 276-286, 2016.

[15] L. Shi, S. Guo, K. Asaka, "A novel multifunctional underwater microrobot," *2010 IEEE International Conference on Robotics and Biomimetics (ROBIO)*, pp. 873-878, 2010.

[16] T. Nagai, and J. Shintake, "Rolled Dielectric Elastomer Antagonistic Actuators for Biomimetic Underwater Robots," *Polymers,* vol.14, no. 21, pp. 4549, 2022.

[17] N. Graf, A. Behr and K. Daltorio, "Crab-Like Hexapod Feet for Amphibious Walking in Sand and Waves," *Biomimetic and Biohybrid Systems,* vol.11556, no. 7, pp. 158-170, 2019.

[18] R. Baines, J. Booth, F. Fish and R. Kramer-Bottiglio, "Toward a bio-inspired variable-stiffness morphing limb for amphibious robot locomotion," *2019 2nd IEEE International Conference on Soft Robotics (RoboSoft)*, pp. 704-710, 2019.

[19] Y. Li, S. Guo, and C. Yue, "Preliminary concept and kinematics simulation of a novel spherical underwater robot," *IEEE International Conference on Mechatronics & Automation*, pp. 1907-1912, August 2015.

[20] H. Xing, S. Guo, L. Shi, X. Hou, Y. Liu and H. Liu, "Design, modeling and experimental evaluation of a legged, multivectored water-jet composite driving mechanism for an amphibious spherical robot," *Microsystem Technologies*, vol. 26, no.2, pp. 475-487, July 2020.

[21] J. Yu, R. Ding, Q. Yang, M. Tan, W. Wang, and J. Zhang, "On a bio-inspired amphibious robot capable of multimodal motion," *IEEE/ASME transactions on mechatronics*, vol. 17, no.5, pp. 847-856, May 2012.

[22] L. Shi, P. Bao, S. Guo, Z. Chen and Z. Zhang, "Underwater formation system design and implement for small spherical robots," *IEEE Systems Journal*, vol. 17, no. 1, pp. 1259-1269, March 2023.

[23] P. Bao, Y. Hu, L. Shi, S. Guo and Z. Li, "A decoupling three-dimensional motion control algorithm for spherical underwater robot," *Biomimetic Intelligence and Robotics,* vol. 2, no. 3, pp. 100067, September 2022.

[24] G. Chen, J. Tu, X. Ti, Z. Wang, and H. Hu, "Hydrodynamic model of the beaver-like bendable webbed foot and paddling characteristics under different flow velocities," *Ocean Engineering*, vol. 234, no. 6, pp. 109179, June 2021.

[25] S. Guo, L. Shi, S. Mao, and M. Li, "Design and kinematic analysis of an amphibious spherical robot," *IEEE International Conference on Mechatronics & Automation*, pp 2214–2219, 2014.

[26] Z. Du, and Y. Yu, "Research on dynamic stress and endurance characteristics of flexible robots," *China Mechanical Engineering*, vol. 29, no. 24, pp. 2985-2989, December 2007.

[27] S. Guo, Y. He, L. Shi, S. Pan, K. Tang, R. Xiao, and P. Guo. "Modal and fatigue analysis of critical components of an amphibious spherical robot," Microsystem Technologies, vol. 23, no. 6, pp. 2233-2247, June 2017.

[28] Y. Zhu, J. Zhang, J. Wang, Z. Shang, "Modal and fatigue analysis of assisted exoskeleton robot based on finite element method," Science Technology Engineering, vol. 20, no. 17, pp. 6916-6922, June 2020.

[29] S. Nie, Y. Li, S. Guo, S. Tao, and F. Xi, "Modeling and simulation for fatigue life analysis of robots with flexible joints under percussive impact forces," *Robotics and Computer Integrated Manufacturing*, vol. 37, no. 1, pp. 292-301, February 2016.

[30] P. Zhi, Y. Li, B. Chen, X. Bai, and Z. Sheng, "Fuzzy design optimization-based fatigue reliability analysis of welding robots," *IEEE Access*, vol. 8, pp. 64906-64917, March 2020.

[31] S. Guo, Z. Li, L. Shi, H. Xing, X. Hou, Y. Liu, H. Liu, Y. Hu and D. Xia, "Basic characteristics evaluation of a duck-like robot," *IEEE International Conference on Mechatronics & Automation*, pp. 1502-1507, 2019.

[32] Z. Li, "Study on the effect of steel decarburization on its fatigue life," *Materials Research and Application*, vol. 16, no. 5, pp. 854-860, October 2020.